

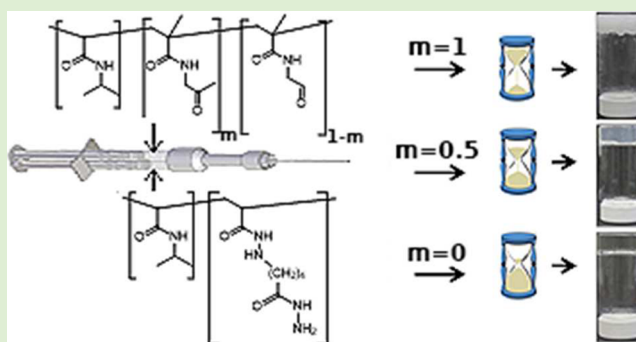
# Tuning Gelation Time and Morphology of Injectable Hydrogels Using Ketone–Hydrazide Cross-Linking

Mathew Patenaude, Scott Campbell, Dennis Kinio, and Todd Hoare\*

Department of Chemical Engineering, McMaster University, 1280 Main Street West, Hamilton, Ontario, Canada L8S 4L7

## Supporting Information

**ABSTRACT:** Injectable, covalently *in situ* forming hydrogels based on poly(*N*-isopropylacrylamide) have been designed on the basis of mixing hydrazide-functionalized nucleophilic precursor polymers with electrophilic precursor polymers functionalized with a combination of ketone (slow reacting) and aldehyde (fast reacting) functional groups. By tuning the ratio of aldehyde:ketone functional groups as well as the total number of ketone groups in the electrophilic precursor polymer, largely independent control over hydrogel properties including gelation time (from seconds to hours), degradation kinetics (from hours to months), optical transmission (from 1 to 85%), and mechanics (over nearly 1 order of magnitude) can be achieved. In addition, ketone-functionalized precursor polymers exhibit improved cytocompatibility at even extremely high concentrations relative to polymers functionalized with aldehyde groups, even at 4-fold higher functional group densities. Overall, increasing the ketone content of the precursor copolymers can result in *in situ*-gellable hydrogels with improved transparency and biocompatibility and equivalent mechanics and stimuli-responsiveness while only modestly sacrificing the speed of gel formation.



## INTRODUCTION

Hydrogels have attracted widespread interest as biomaterials due to their analogous interfacial, mechanical, and physicochemical properties to many soft tissues.<sup>1</sup> By controlling the chemistry of the monomers or linear polymers used to prepare the hydrogels, the properties of the hydrogels can readily be engineered to optimize their utility as drug storage and release depots,<sup>2</sup> network scaffolds for tissue engineering applications,<sup>3–7</sup> and biosensors.<sup>8–10</sup> Hydrogels cross-linked via covalent bond formation are particularly attractive in that they generally possess more elastic mechanical properties and more tunable degradation kinetics than physically cross-linked hydrogel formulations,<sup>11</sup> making them more suitable within the body for long-term use (especially in applications in which the gels are designed as space-filling or must bear some load). However, this enhanced elasticity makes most chemically cross-linked hydrogels unsuitable for introduction within the body through minimally invasive means such as via injection, requiring invasive surgical implantation that renders them nonideal for routine clinical use.<sup>12</sup> In response, in recent years, a great deal of attention has been drawn toward the development of injectable hydrogels, including physically cross-linked shear thinning hydrogels<sup>13</sup> and chemically cross-linked gels that can form *in vivo* following co-injection of complementary reactive polymer precursors.<sup>13–16</sup> To maintain the advantages of chemically cross-linked hydrogels in the context of injectable formulations, a number of cross-linking chemistries that occur rapidly in water under physiological

conditions have been developed, including Michael-type addition between a thiol-functionalized precursor and  $\alpha,\beta$ -unsaturated acid moieties of another precursor,<sup>17–20</sup> Diels–Alder “click” chemistry between reactive precursors functionalized with furan or maleimide groups,<sup>21–23</sup> oxime formation between a carbonyl group and a hydroxylamine,<sup>24</sup> and Schiff base formation between polymer precursors functionalized with carbonyl and amine functional groups.<sup>25,26</sup> Of particular interest, hydrazone bond formation, resulting from the condensation of carbonyl and hydrazide functional groups, has been widely reported for use with injectable hydrogels due to the rapid kinetics of this chemistry in aqueous environments and the hydrolytic lability of the formed hydrazone group that facilitates both *in situ* formation and biodegradation.<sup>27</sup> We have previously reported the use of this chemistry to prepare injectable environmentally responsive hydrogels based on poly(*N*-isopropylacrylamide) (PNIPAM) that can be tailored to suit a number of biomedical applications, including drug delivery and tissue engineering.<sup>12–14</sup>

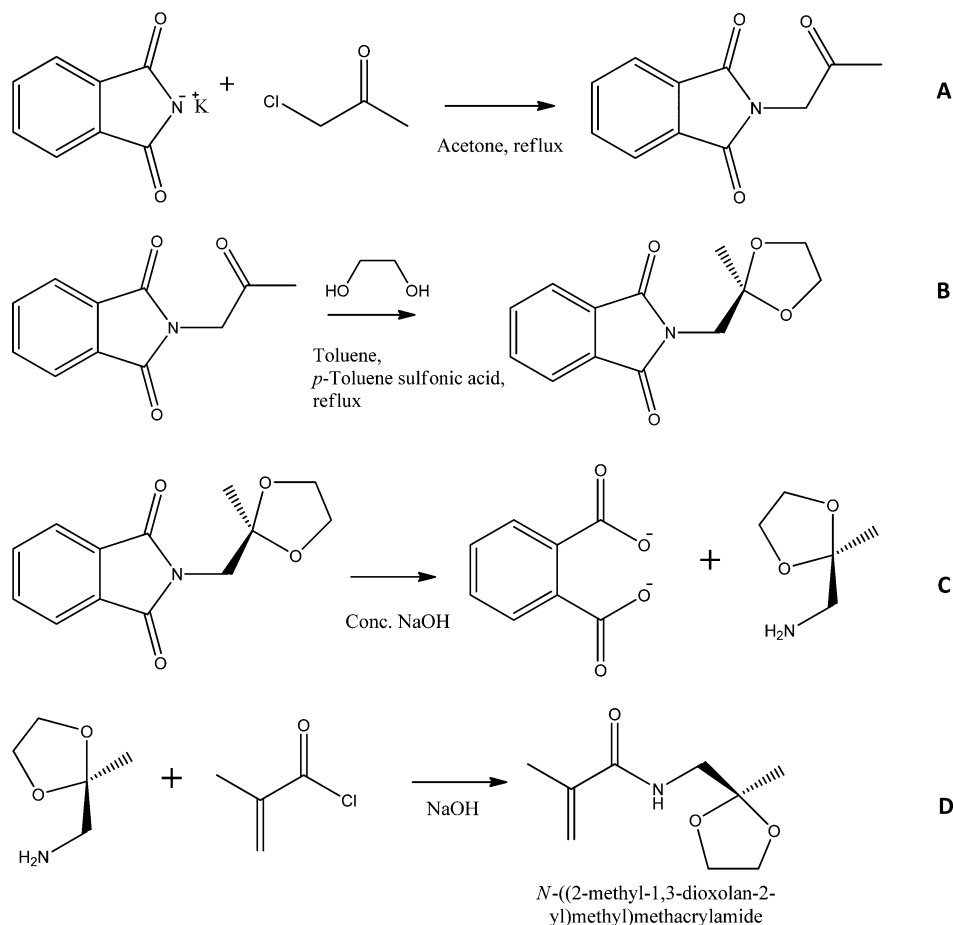
An ideal hydrogel chemistry for most tissue engineering or drug delivery applications would facilitate moderate to rapid rates of gel formation (preventing or minimizing undesirable diffusion of the precursor polymers away from the injection site prior to gel formation), form hydrogels with degradable

Received: November 1, 2013

Revised: January 2, 2014

Published: January 16, 2014

Scheme 1. Synthesis of a Ketal-Protected Ketone Monomer



linkages, and avoid reactions with biomolecules in the gel environment. In the latter case, ensuring self-gelation instead of cross-reaction of the gel precursors with biomolecules is critical to produce hydrogels with sufficiently high cross-link densities (i.e., adequate mechanics) as well as prevent or suppress potential reactions with proteins, which can lead to significant inflammatory responses.<sup>28</sup> However, most if not all existing chemistries reported in the literature present limitations with respect to at least one of these criteria. For example, aldehyde groups employed in generating hydrazone cross-linked hydrogels can induce local toxicity if used at high concentrations or with sterically hindered polymers which gel more slowly (inducing effective rapid release of aldehyde polymers into the body) due to their ability to cross-link proteins via their lysine groups.<sup>29,30</sup> In addition, from a fundamental engineering perspective, current gelation chemistries are inherently limited in that the cross-link density, gelation rate, mechanics, and degradation time of the hydrogel are all intimately coupled; hydrogels with higher cross-linking potential gel faster and form gels that are more elastic and degrade more slowly.<sup>11</sup> Gelation kinetics and the final morphology of the hydrogel are also often linked given that rapid cross-linking reactions can induce gelation faster than the time scale required for diffusional mixing of precursor polymers. As a result, depending on the type of mechanical mixing used during the gel formation process, regions of local heterogeneity may form within the polymer matrixes of these gels that scatter light (significantly affecting the utility of these gels in ophthalmic applications,<sup>31</sup> for example), alter the diffusional properties of small molecules

through the gel, and/or degrade the mechanical properties of the gel. Finding ways to decouple these variables, in particular gelation time with mechanics and degradation rate, would greatly improve our ability to engineer specific hydrogels for particular biomedical applications.

Recent approaches to addressing this problem have involved changing the chemical characteristics of the electrophile to alter hydrogel properties. In particular, McKinnon et al. demonstrated that using an aryl aldehyde instead of an aliphatic aldehyde can be used to alter the properties of the hydrogel formed.<sup>32</sup> In this work, we seek to address these challenges by using ketone groups (alone or in combination with aldehyde groups) as the electrophilic reactive group used to form the hydrazone cross-link. Ketones are less reactive to hydrazone bond formation than aldehydes,<sup>33</sup> attributable to the presence of an extra electron-donating carbon at the  $\alpha$  position of the carbonyl group as well as steric hindrance to nucleophilic attack of the carbonyl group. By adjusting the total number of ketone groups as well as the aldehyde:ketone ratio in the electrophilic precursor polymer, we aim to engineer the gelation time to produce a range of hydrogels with tunable properties. To demonstrate this phenomenon, we have chosen poly(*N*-isopropylacrylamide) (PNIPAM) as the backbone polymer for gel formation. PNIPAM has attracted significant interest in the biomedical literature due to its ability to respond to the temperature of its local environment; PNIPAM hydrogels undergo a reversible volume phase transition at  $\sim 32$  °C that results in significant and reversible swelling within the hydrogel matrix.<sup>34</sup> This environmental sensitivity allows for

the design of gels that can both reduce their pore size as well as switch from highly hydrophilic to partially hydrophobic on demand to (for example) entrap preloaded drug and slow its release<sup>35</sup> or adhere and then release cells for regenerative medicine applications.<sup>36</sup> We have previously demonstrated the fabrication of PNIPAM hydrogels using aldehyde–hydrazide chemistry.<sup>16</sup> While gels with suitable mechanical and thermoresponsive properties were produced, the gels formed very quickly (~10–30 s, problematic in some surgical contexts) and were extremely opaque. Herein, by using ketone groups to tune the gelation kinetics, we demonstrate the potential to create transparent but still mechanically strong and highly thermoresponsive hydrogels based on PNIPAM precursors.

## EXPERIMENTAL SECTION

**Materials.** *N*-Isopropylacrylamide (NIPAM, 99%), acrylic acid (AA, 99%), adipic acid dihydrazide (ADH, 98%), *N*'-ethyl-*N*-(3-dimethylaminopropyl)-carbodiimide (EDC, commercial grade), ethylene glycol (99.8%), thioglycolic acid (MAA, ≥98.0%), toluene (99.8%), acetone (anhydrous, ≥99.9%), chloroacetone (95%), phthalimide potassium salt (≥98%), methacryloyl chloride (≥97.0%), aminoacetaldehyde dimethyl acetal (99%), 4-hydroxy-TEMPO (97%), and *para*-toluenesulfonic acid (≥98.5%) were all purchased from Sigma Aldrich (Oakville, ON). Dimethyl sulfoxide (DMSO, reagent grade) was purchased from Caledon Laboratory Chemicals (Georgetown, ON). 3T3 *Mus musculus* mouse cells were obtained from ATCC: Cederlane Laboratories (Burlington, ON). Cell proliferation media (which includes Dulbecco's modified Eagle's medium-high glucose (DMEM), fetal bovine serum (FBS), and penicillin streptomycin (PS)), trypsin-EDTA, and recovery media were all acquired from Invitrogen (Burlington, ON).

**Synthesis of an Acetal-Protected Aldehyde Monomer (*N*-(2,2-Dimethoxyethyl)methacrylamide).** Aminoacetaldehyde dimethyl acetal (50 mL, 46 mmol) was added to a 120 mL stirred solution of 20% NaOH (w/v). This solution was then cooled to 0 °C in an ice bath. 4-Hydroxy TEMPO (10 mg, 0.06 mmol) was then added to this solution as a stabilizer and stirred until it was fully dissolved in solution. Methacryloyl chloride (47 mL, 48 mmol) was next added dropwise over the course of 2 h under nitrogen flow, after which the ice bath was allowed to warm to room temperature and the reaction was left to stir overnight in darkness. The reaction mixture was then extracted with 150 mL of petroleum ether. Subsequently, the aqueous phase was saturated with sodium chloride and was extracted three times with *tert*-butyl methyl ether. Additional 4-hydroxy TEMPO was added to this phase to prevent premature polymerization of the monomer. The organic phase was then dried over magnesium sulfate, filtered, and concentrated in a rotary evaporator, yielding the acetal-protected aldehyde monomer. The monomer was stored in the darkness at –20 °C until use. <sup>1</sup>H NMR (600 MHz) in DMSO-*d*<sub>6</sub>: CH<sub>2</sub>CCH<sub>3</sub>COONHR', 1.75 ppm, singlet, 3H; RNHCH<sub>2</sub>CH(OCH<sub>3</sub>)<sub>2</sub>, 3.25 ppm, triplet, 1H; RNHCH<sub>2</sub>CH(OCH<sub>3</sub>)<sub>2</sub>, 3.35 ppm, singlet, 6H; RNHCH<sub>2</sub>CH(OCH<sub>3</sub>)<sub>2</sub>, 4.41 ppm, doublet, 2H; CH<sub>2</sub>CCH<sub>3</sub>COONHR', 5.35–5.65 ppm, doublet, 2H; RNHR', 8 ppm, singlet, 1H (see the Supporting Information, Scheme S1).

**Synthesis of a Ketal-Protected Ketone Monomer (*N*-(2-Methyl-1,3-dioxolan-2-yl)methyl)methacrylamide.** Synthesis of the protected ketone monomer was conducted on the basis of a modification of a previously reported protocol.<sup>37</sup> Chloroacetone (10 mL, 12.5 mmol) and the potassium salt of phthalimide (25.5 g, 13.8 mmol) were added to 150 mL of stirred dry acetone. The solution was then heated to 80 °C for 20 h, after which it was cooled to room temperature and the acetone was removed in a rotary evaporator. The resulting solid was then redissolved in methylene chloride and washed repeatedly with water. The methylene chloride layer was dried over magnesium sulfate, filtered, and removed using a rotary evaporator. The resulting yellow crude solid was washed with diethyl ether several times until the solid became white; this solid was subsequently dried in a vacuum oven to yield purified intermediate A (Scheme 1A).

Intermediate A (10 g, 50 mmol) was then added to 180 mL of toluene along with ethylene glycol (5.85 mL, 100 mmol) and dry *para*-toluenesulfonic acid (934 mg, 5 mmol) and refluxed for 15 h. The reaction mixture was cooled to room temperature, and the ethylene glycol layer was extracted three times with diethyl ether. The toluene and ether fractions were combined and washed three times with 5% (w/v) NaOH followed by deionized water. The organic layer was dried over magnesium sulfate, and solvent was removed in a rotary evaporator. The crude was recrystallized from ethanol to yield pure intermediate B (Scheme 1B). Intermediate B was subsequently added to 100 mL of deionized water along with 15 g of NaOH and refluxed for 2 days, with an additional 60 g of NaOH added slowly over the course of the reflux. Afterward, the reaction mixture was cooled to room temperature and extracted three times with 50 mL of dichloromethane. The organic layers were then combined and dried over magnesium sulfate, filtered, and concentrated in a rotary evaporator to yield pure product C (Scheme 1C), a slightly yellow oil. Finally, the monomer was prepared by adding product C (21.1 mL, 180 mmol) to a 20% (w/v) NaOH solution (in water) containing 4-hydroxy TEMPO (10 mg, 0.06 mmol). This reaction mixture was brought to 0 °C in an ice bath, and methacryloyl chloride (16.5 mL, 174 mmol) was added dropwise over 2 h under nitrogen flow. The ice bath was then allowed to warm to room temperature and the reaction left to stir overnight in darkness. After this time, stirring was halted and the product was allowed to collect at the top of the reaction flask. The pure monomer product (along with inhibitor) (shown in Scheme 1D) was then isolated using a separatory funnel. The monomer was stored in the darkness at –20 °C until use. <sup>1</sup>H NMR (600 MHz) in DMSO-*d*<sub>6</sub>: RNHCH<sub>2</sub>C(OCH<sub>2</sub>CH<sub>2</sub>O)CH<sub>3</sub>, 1.3 ppm, singlet, 3H; CH<sub>2</sub>CCH<sub>3</sub>CONHR', 2 ppm, singlet, 3H; RNHCH<sub>2</sub>C(OCH<sub>2</sub>CH<sub>2</sub>O)CH<sub>3</sub>, 3.5 ppm, doublet, 2H; RNHCH<sub>2</sub>C(OCH<sub>2</sub>CH<sub>2</sub>O)CH<sub>3</sub>, 4 ppm, singlet, 4H; CH<sub>2</sub>CCH<sub>3</sub>CONHR', 5.35–5.65 ppm, doublet, 2H; CH<sub>2</sub>CCH<sub>3</sub>CONHR', 6 ppm, singlet, 1H. See the Supporting Information, Figure S1, for the <sup>1</sup>H NMR spectrum.

**Synthesis of Hydrazide-Functionalized PNIPAM Copolymer.** The synthesis of this nucleophilic copolymer was performed as previously described<sup>16</sup> (see also the Supporting Information, Scheme S2). Briefly, *N*-isopropylacrylamide (4 g, 35 mmol), acrylic acid (1 mL, 14 mmol), and thioglycolic acid (87 μL, 1.25 mmol) were dissolved in 20 mL of absolute ethanol and heated to 56 °C. Following degassing with nitrogen, dimethyl 2,2'-azobis(2-methylpropionate) (AIBME) (56 mg, 2.4 μmol) was added, and the solution was allowed to stir overnight under nitrogen. The solvent was then removed in a rotary evaporator, and the crude product was redissolved in deionized water and subjected to exhaustive dialysis followed by lyophilization. Conductometric titration (ManTech, Inc.) indicated that the copolymer contained 15.2 ± 0.4 mol % acrylic acid residues per chain. The acrylic acid residues were then converted to hydrazide groups by dissolving the polymer in deionized water along with a 10-fold molar excess of ADH and adjusting the solution pH to 4.75 using 0.1 M HCl. A 2-fold molar excess of EDC (predissolved in 10 mL of deionized water) was then added to the solution, and the reaction was allowed to continue (maintaining a constant pH of 4.75 throughout the reaction via addition of 0.1 M HCl) until no change in pH was observed, typically on the order of ~4 h. At this point, the solution was neutralized using 0.1 M NaOH and subjected to exhaustive dialysis and subsequent lyophilization. Conductometric titration indicated that 97 ± 3% of acrylic acid groups had been converted to hydrazide groups, resulting in ~14.7 mol % hydrazide groups per PNIPAM copolymer chain. DMF gel permeation chromatography was conducted using a Waters 590 HPLC pump along with three Waters Ultrastaygel Linear columns operating in series and a Waters 410 refractive index detector. GPC indicated a number average molecular weight of 26.5 kDa (polydispersity 1.55) for this hydrazide-functionalized copolymer based on narrow molecular weight polyethylene glycol standards (Waters).

**Synthesis of Aldehyde- and/or Ketone-Functionalized PNIPAM Copolymers.** *N*-Isopropylacrylamide (4 g, 35 mmol) was copolymerized with various ratios of protected aldehyde to protected ketone monomer (Scheme 2), keeping the total mole percent of these

**Scheme 2. Synthesis of Protected Ketone and/or Aldehyde Monomers with NIPAM and Subsequent Deprotection to Reveal the Electrophilic Ketone and/or Aldehyde Moieties**

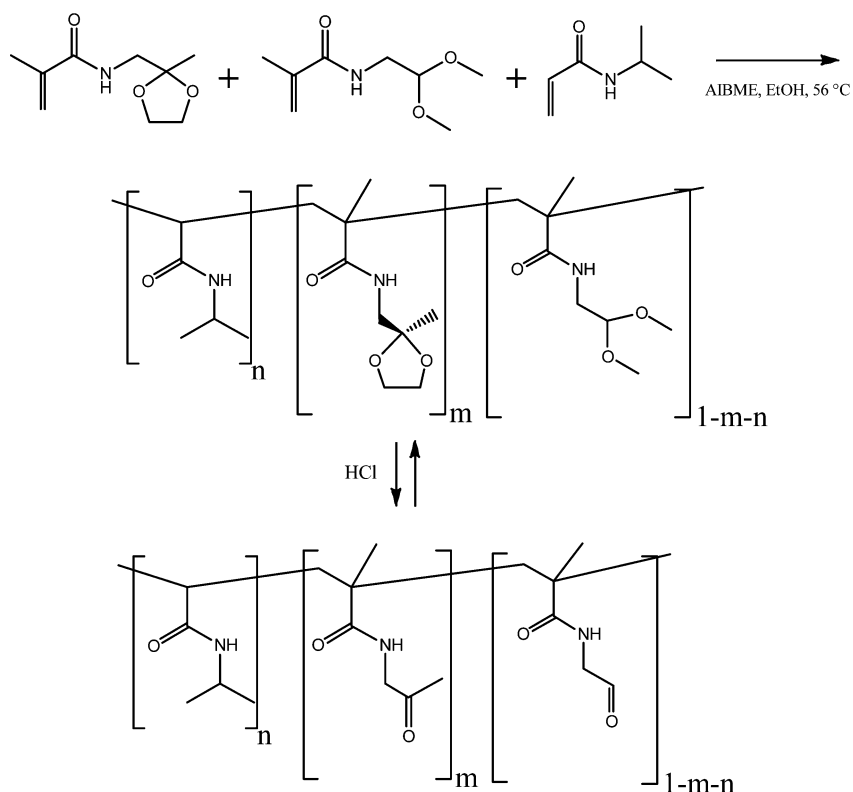


**Table 1. Compositions and Properties of Electrophilic PNIPAM Copolymer Chains<sup>a</sup>**

| gel identification | aldehyde content ( $X_{na}$ ) | ketone content ( $X_{nk}$ ) | total electrophile content ( $X_n$ ) | total NIPAM content ( $X_{nip}$ ) | $M_w$ (kDa)    |
|--------------------|-------------------------------|-----------------------------|--------------------------------------|-----------------------------------|----------------|
| 100Ald/0Ket        | 1                             | 0                           | $0.12 \pm 0.03$                      | $0.88 \pm 0.03$                   | $21.2 \pm 3.2$ |
| 75Ald/25Ket        | $0.72 \pm 0.05$               | $0.28 \pm 0.05$             | $0.11 \pm 0.02$                      | $0.89 \pm 0.02$                   | $20.4 \pm 2.3$ |
| 50Ald/50Ket        | $0.45 \pm 0.07$               | $0.55 \pm 0.07$             | $0.11 \pm 0.04$                      | $0.89 \pm 0.04$                   | $21.8 \pm 3.3$ |
| 25Ald/75Ket        | $0.23 \pm 0.03$               | $0.77 \pm 0.03$             | $0.13 \pm 0.03$                      | $0.87 \pm 0.03$                   | $22.5 \pm 2.1$ |
| 0Ald/100Ket        | 0                             | 1                           | $0.12 \pm 0.05$                      | $0.88 \pm 0.05$                   | $20.6 \pm 1.9$ |
| 0Ald/100Ket*       | 0                             | 1                           | $0.42 \pm 0.05$                      | $0.58 \pm 0.05$                   | $19.5 \pm 2.6$ |

<sup>a</sup>The gel identification codes represent the anticipated mole fractions of the aldehyde:ketone monomers based on the recipe, while the actual mole fractions of aldehyde and ketone functional groups within the polymer chains (as determined by <sup>1</sup>H NMR) are given as  $X_{na}$  and  $X_{nk}$ , respectively. The mole fractions of monomer types, either electrophilic monomer or NIPAM, are given as  $X_n$  and  $X_{nip}$ , respectively. GPC results are reported relative to a polyethylene glycol standard curve.

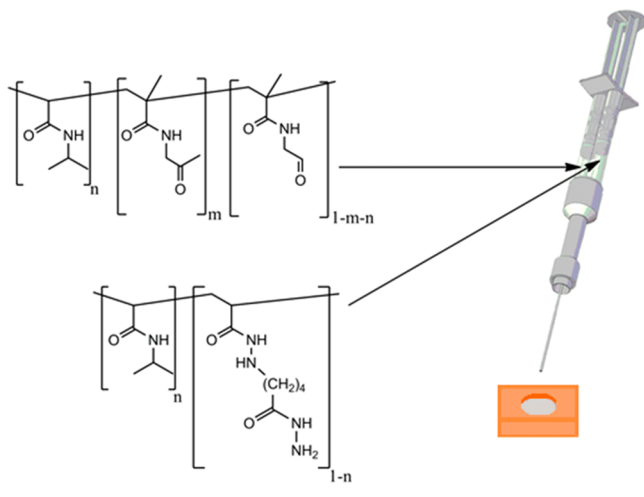
protected functional groups (and thus electrophilic reactive groups for covalent gelation) constant. The recipes used to prepare these ketone- and/or aldehyde-functionalized copolymers are given in Table 1. The polymerizations were carried out as described for the hydrazide-containing copolymer. Following removal of ethanol with a rotary evaporator, the protecting acetal and ketal groups were removed by redissolving the obtained crude polymer in 3 M HCl and allowing the resulting solution to stir at room temperature for 24 h. This solution was then exhaustively dialyzed and lyophilized to isolate the purified copolymers. Aldehyde and ketone group content was quantified via NMR by measuring the relative peak intensity at 9.5 ppm (RCOH, aldehyde) and 2.1 ppm (RCOCH<sub>3</sub>, ketone) relative to a tetramethylsilane internal standard. GPC was performed as previously described for the hydrazide-functionalized copolymer.

**Hydrogel Formation, Gelation Time, and Transparency Assays.** Hydrazide (nucleophilic) and aldehyde/ketone (electrophilic) functionalized polymer precursors were dissolved separately in PBS at 25 °C at a concentration of 6% (m/v) for each precursor polymer and added to separate barrels of a double barrel syringe (Scheme 3). Depressing the plunger of the syringe caused the polymer precursors to mix along a baffled channel and co-extrude out of the tip

of a needle. The time required to form a stable gel was assessed using a standard vial inversion technique following co-extrusion of the reactive polymer precursors into a 20 mL glass scintillation vial.<sup>21,38,39</sup> The time required to form a gel (i.e., the time required such that the polymer did not flow within 5 s following vial inversion) was noted for each gel type. In order to assess the potential formation of microdomains and/or phase separation, gels were formed in polystyrene cuvettes (1 cm path length) and the transparency of the resulting gels was measured at 550 nm using a DU 800 UV/visible spectrophotometer (Beckman Coulter) following 24 h of incubation at room temperature. The phosphate buffer maintained the pH at 7.4 in all gelation experiments. A total of  $n = 4$  replicates were performed per sample in each assay, with the reported error bars representing the standard deviation of the measurements.

**Hydrogel Cross-Linking Efficiency.** Polymer precursors 100Ald/0Ket, 50Ald/50Ket, 0Ald/100Ket, and 0Ald/100Ket\* were dissolved in D<sub>2</sub>O at 6% (m/v) and were added to one barrel of different double barrel syringes. A 6% (w/v) solution of hydrazide-functionalized PNIPAM in D<sub>2</sub>O was then added to the second barrel of each of these syringes, and hydrogels were made by co-extruding each polymer pair into different NMR tubes. Spectral measurements were taken

### Scheme 3. Co-Injection of Hydrazide and Aldehyde/Ketone Complementary PNIPAM Precursors into a Silicone Mold Using a Double Barrel Syringe to Form a Hydrazone Cross-Linked Hydrogel



immediately following co-extrusion into the tubes for each gel type as well as 48 h after co-extrusion (allowing cross-linking to occur). Changes in peak intensity corresponding to aldehyde protons (COH,  $\sim 9.5$  ppm) and terminal methyl groups of ketone moieties (CH<sub>3</sub>,  $\sim 2.15$  ppm), both of which decrease following hydrazone bond formation, were tracked relative to spectra of polymer precursors alone at a total concentration of 3% (matching the concentration of each precursor in each final gel) in D<sub>2</sub>O. Sixteen scans were taken for each sample type at a relaxation delay of 4 s per scan. The ratio of peak integrations relative to the isopropyl group intensity of NIPAM moieties was measured for both precursor alone and co-extruded polymer solutions and compared at different time points in the experiment (initially and at 48 h). For 50Ald/50Ket gels, measurements were taken for both aldehyde and ketone functional groups independently of each other, allowing for the calculation of the total residual electrophilic group content in the gel. Quantification of the number of electrophilic groups (of a given type) consumed through cross-linking was made according to eq 1

$$\% \text{ electrophilic groups consumed} = \left( 1 - \frac{I_{e,g}/I_{i,g}}{I_{e,s}/I_{i,s}} \right) \times 100\% \quad (1)$$

where  $I_{e,g}$ ,  $I_{i,g}$ ,  $I_{e,s}$ , and  $I_{i,s}$  are the integrations corresponding to the electrophilic (ketone or aldehyde) peaks of the gel after 48 h, the isopropyl groups of the gel after 48 h, the electrophilic peaks of the polymer precursor solution initially ( $t = 0$ ), and the isopropyl groups of the polymer precursor solution initially ( $t = 0$ ), respectively.

**Hydrogel Degradation.** Hydrogel precursor solutions were co-extruded into 0.44 mL silicone molds, as shown in Scheme 3. The solution-containing molds were then covered with silicone slabs and left for 48 h at room temperature in order to ensure equilibrium cross-linking of the polymer networks. Hydrogels were then placed in cell culture inserts (12-well format, Falcon) and were subsequently submerged in PBS at pH 7.4. The rates of degradation for each gel type were determined gravimetrically at predetermined time intervals after drawing off excess (unbound) water from the surface of the gels using a Kimwipe. A total of  $n = 4$  replicates are performed on each sample, with the reported error bars representing the standard deviation of the measurements.

**Hydrogel Mechanical Properties.** The mechanical properties of hydrogels formed by co-extruding hydrazide-functionalized PNIPAM and PNIPAM functionalized with different ratios of ketones to aldehydes were determined using oscillatory rheology with an ARES rheometer (Texas Instruments). The storage modulus ( $G'$ ) of each gel

type was determined using parallel plate geometry with a plate diameter of 7 mm and a plate spacing of 1 mm. An initial strain sweep was first conducted between 1 and 100% at 1 Hz in order to identify the linear viscoelastic range of these gels. A strain within this linear viscoelastic range was then selected and maintained constant during a frequency sweep from 1 to 100 rad/s to measure  $G'$ . Measurements were performed on gels initially incubated at room temperature and at 37 °C. A total of  $n = 4$  replicates are performed on each sample, with the reported error bars representing the standard deviation of the measurements.

**Cytocompatibility Assays.** The cytocompatibility of the hydrogel precursors (which are also the degradation products)<sup>16</sup> was assessed using an *in vitro* MTT assay with 3T3 *Mus musculus* mouse cells similar to that described by Campbell et al.<sup>14</sup> Briefly, 24-well polystyrene plates were cultured with 10 000 3T3 cells within 1 mL of proliferation media. After 24 h, the cells were exposed to various concentrations of hydrogel precursor polymers (0.1, 0.4, 0.8, 1.2, 1.6, and 2 mg/mL for the lower concentration sets and 2, 4, 8, 12, 16, and 20 mg/mL for the higher concentration set,  $n = 4$  per concentration) and incubated for an additional 24 h. The media and polymer solutions were replaced with 1 mL of a 0.4 mg/mL MTT solution in proliferation media for the last 3 h of incubation. After this, the MTT solution was aspirated off and the formazan produced by the cells was dissolved in 400  $\mu$ L of DMSO. The absorbance of the formazan solution was read using a Biorad microplate reader (model 550) at 570 nm against a 630 nm baseline (accounting for media absorbance) and compared to the absorbances measured in cell-only wells in which no material (i.e., only media) was added to calculate the relative cell viabilities according to eq 2.

$$\text{cell viability (\%)} = \frac{(\text{absorbance}_{\text{polymer-exposed},570\text{nm}} - \text{absorbance}_{\text{polymer-exposed},630\text{nm}})}{(\text{absorbance}_{\text{blank},570\text{nm}} - \text{absorbance}_{\text{blank},630\text{nm}})} \quad (2)$$

Error bars for each polymer tested represent the standard deviation of the cell viability percentages measured for the four replicates performed. A Student's  $t$  test (at 95% confidence) is performed to assess the statistical significance of differences between cell viability results.

## RESULTS

**Reactive Precursor Polymer Synthesis.** As per Table 1, an approximately stoichiometric incorporation of monomers at their desired mole fractions within each polymer chain was obtained for both the ketal- and acetal-protected monomers, resulting in electrophilic polymer chains with statistically equal functional group contents (and therefore cross-linking potential) in all hydrogels studied. For an equal mass mixture of the polymers (each at 6%), the hydrazide polymers contain functional groups in approximately a 1.5-fold excess over electrophilic groups on complementary precursor polymer chains, advantageous biologically given that hydrazides are functionally bio-orthogonal with biomolecule functional groups, whereas aldehydes and, to a much lesser extent, ketones are not. The  $\sim 42$  mol % 0Ald/100Ket\* electrophilic polymer is the exception to this relationship and is designed to offer enhanced gel formation kinetics and cross-link density relative to the other precursor polymers prepared. The molecular weight of each electrophilic precursor polymer was maintained at  $\sim 20$  kDa (independent of functional group incorporation, Table 1), while the nucleophilic chain had a molecular weight of 26.5 kDa. Considering that hydrazone bond hydrolysis regenerates the precursor polymers (i.e., the precursor polymers are the degradation products), each tested polymer has a molecular weight below the lower molecular weight cutoff of the glomerulus basement membrane of the renal excretory system

(~40 kDa) and thus has the potential to be cleared following degradation.

**Hydrogel Formation Kinetics.** Hydrogels prepared with any combination of aldehyde/ketone functionalization could be easily co-extruded from a double-barrel syringe, and all combinations tested successfully gelled within the silicone molds to form elastic hydrogels within the 24 h gelation period used for screening. Results of the vial inversion assay, shown in Table 2, indicate that an increase in ketone content of the

**Table 2. Time Required to Form a Hydrogel for the Various Gel Types Assayed According to the Vial Inversion Test**

| gel ID       | gel formation time (min) |
|--------------|--------------------------|
| 100Ald/0Ket  | 0.09 ± 0.02              |
| 75Ald/25Ket  | 0.4 ± 0.1                |
| 50Ald/50Ket  | 24 ± 2                   |
| 25Ald/75Ket  | 45 ± 6                   |
| 0Ald/100Ket  | 65 ± 13                  |
| 0Ald/100Ket* | 2.0 ± 0.5                |

electrophilic polymer leads to an increase in the time required to form a gel, with the gelation time increasing dramatically when the ketone concentration is increased to >50 mol %.

This increased gelation time associated with ketone-rich polymers can be attributed to the lower electrophilicity of the ketone group relative to the aldehyde group, making ketones less susceptible to nucleophilic attack by the hydrazide-functionalized PNIPAM chains. When the number of ketone groups in the precursor polymers is quadrupled to ~42 mol % (0Ald/100Ket\*), gelation occurs 30-fold faster than when a ~12 mol % ketone-functionalized precursor polymer is used (0Ald/100Ket). Interestingly, the gelation time observed using the ~42 mol % ketone-functionalized precursor is still ~20-fold slower than that observed when using an aldehyde-functionalized polymer with ~12 mol % functional groups to form gels.

**Hydrogel Cross-Linking Efficiency.** By comparing the aldehyde and ketone group NMR spectral intensities immediately following co-extrusion and 48 h postextrusion, an estimate of the cross-link density of the respective hydrogels can be made. Changes in peak intensities were measured relative to 3% (w/v) solutions of precursor only in D<sub>2</sub>O (see representative raw data spectra in the Supporting Information, Figures S2 and S3). Table 3 shows the percentage of ketone and/or aldehyde functional groups consumed in each gel as a function of precursor chemistry and the total cross-link density of each hydrogel following 48 h of gel formation.

Hydrogels prepared with aldehyde-rich precursor polymers contain significantly more cross-links relative to those prepared with ketone-rich precursor polymers at the same total

**Table 3. Electrophilic Functional Group Consumption and Cross-Link Density for Hydrogels Prepared with Different Aldehyde:Ketone Ratios and Total Ketone Contents as Determined by <sup>1</sup>H NMR**

| hydrogel ID  | % electrophilic functional groups consumed | no. of electrophilic functional groups consumed ( $\times 10^{18}$ ) | cross-link density ( $\times 10^{18} \text{ cm}^{-3}$ ) |
|--------------|--|--|---|
| 100Ald/0Ket  | 74 ± 6                                     | 22.4 ± 1.8   | 11.2 ± 0.9  |
| 50Ald/50Ket  | 42 ± 5                                     | 12.3 ± 1.4   | 6.1 ± 0.7   |
| 0Ald/100Ket  | 14 ± 3                                     | 3.9 ± 0.5  | 1.9 ± 0.2   |
| 0Ald/100Ket* | 17 ± 5                                     | 19.3 ± 1.4   | 9.6 ± 0.7   |

electrophile content (~12 mol %), consistent with the higher reactivity of aldehyde groups relative to ketone groups that would shift the equilibrium of hydrazone bond formation/breaking toward the product (cross-linked) side. However, the cross-link density of a gel prepared with an aldehyde-functionalized precursor polymer can be matched using a ketone-functionalized polymer precursor functionalized with a higher total mole fraction of ketone functionality (Table 1). The percentage of available ketone groups cross-linked is approximately equal between the 0Ald/100Ket (~12 mol % ketone) and 0Ald/100Ket\* (~42 mol % ketone) precursors, consistent with an equilibrium driving hydrazone bond formation; however, the 4-fold increase in the total electrophilic functional group content of 0Ald/100Ket\* relative to 0Ald/100Ket results in formation of ~4–5-fold more cross-links in the hydrogel. While it is possible that the absolute extent of cross-linking in (unbuffered) D<sub>2</sub>O will differ from that in (buffered) H<sub>2</sub>O, it is clear from this data that the cross-link density of the hydrogel can be scaled directly by the number of reactive functional groups in the precursor polymers.

**Hydrogel Mechanics.** The results of oscillatory rheometry conducted on a range of hydrogels prepared with precursor polymers containing varying ratios of aldehyde and ketone groups are shown in Figure 1. A clear relationship exists

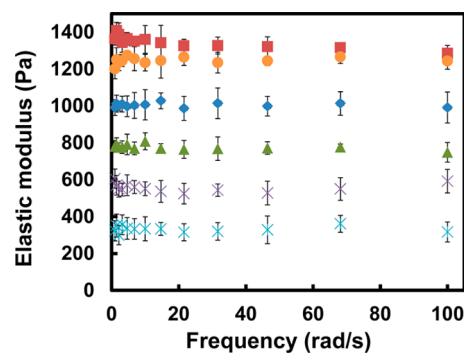


**Figure 1.** Elastic moduli versus frequency for PNIPAM hydrogels prepared with precursor polymers containing different aldehyde:ketone functional group ratios and different ketone functional group mole fractions (0Ald/100Ket\* = ~42 mol % ketones; all other hydrogels ~12 mol % electrophile).

between the elastic modulus ( $G'$ ) and the ratio of aldehyde to ketone groups of the electrophilic precursor polymers used to synthesize the hydrogels, with an increasing aldehyde to ketone ratio yielding gels with an increased  $G'$ . This suggests that aldehydes are significantly more effective at forming cross-links than ketone groups following co-extrusion, consistent with the NMR result (Table 3) and the lower reactivity of ketone functional groups. Interestingly, the 0Ald/100Ket\* hydrogels (prepared with ~42 mol % ketone precursor polymers as opposed to ~12 mol % total electrophilic comonomer precursor polymers used to prepare the other hydrogels) exhibited analogous mechanical properties to the 100Ald/0Ket hydrogel, with the additional available ketone functional groups facilitating an increase in cross-link formation; again, this result matches that of the NMR experiment (Table 3). Thus, while the use of ketone-functionalized polymers results in a significant decrease in the elastic modulus of the resulting hydrogels at equal functional group contents, modulus matching can still be performed independent of the aldehyde:ketone ratio of the reactive copolymers by changing

the total ketone content in the electrophilic hydrogel precursor polymer.

**Hydrogel Transparency.** UV/vis absorbance measurements performed at 550 nm were used to assess the transparency of the hydrogels prepared with the different precursor polymers. A lack of transparency at this wavelength indicates the presence of microdomains of a size similar to the wavelength of the incident light. Figure 2 indicates that

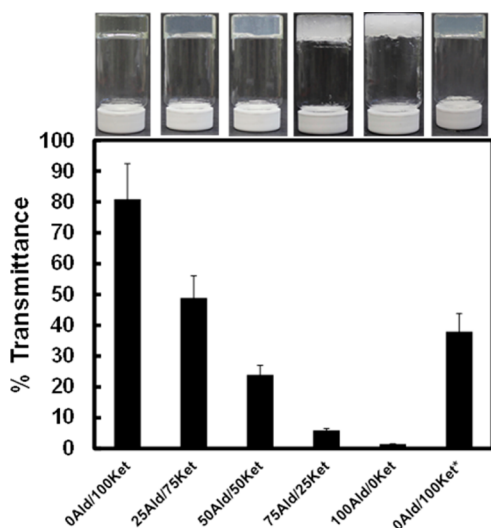


**Figure 2.** Transmittance of 550 nm light through hydrogels prepared with precursor polymers containing aldehyde:ketone functional group ratios and different ketone functional group mole fractions (0Ald/100Ket\*  $\sim$  42 mol % ketones; all other hydrogels = 12 mol % electrophile). Pictures of each hydrogel are provided above each transparency result for reference.

increasing the aldehyde content of the precursor polymers results in significantly less transparent hydrogels, indicating the presence of microdomains and regions of heterogeneity within the bulk gel. Conversely, gels prepared with precursors containing a high fraction of ketone groups remain transparent, with the higher transparency largely preserved as the number of ketone functional groups is increased (comparing 0Ald/100Ket with  $\sim$ 12 mol % ketones and 0Ald/100Ket\* with  $\sim$ 42 mol % ketones); this result suggests that the ketone group itself plays a role in maintaining the gel transparency even independent of the gelation time, since the 0Ald/100Ket\* gel forms 10-fold faster than the 50Ald/50Ket gel but maintains significantly higher transparency.

**Hydrogel Phase Transition.** Incubation of the hydrogels in PBS at 37 °C induced deswelling in all gels, consistent with the phase transition behavior of PNIPAM (Figure 3). Of note, while the precursor polymers themselves are significantly more hydrophilic than PNIPAM (with LCST values of 78 °C for PNIPAM–hydrazide, 45 °C for PNIPAM–aldehyde, and 37 °C for PNIPAM–ketone, with both electrophilic chains possessing  $\sim$ 12 mol % functionalization), the phase transition of the hydrogel occurs at a temperature analogous to that of PNIPAM prepared via standard free radical processes. Similar degrees and kinetics of deswelling are observed across each gel type; however, an increase in ketone content leads to a somewhat higher degree of thermal collapse of the polymer network. This discrepancy between different gel types can be attributed primarily to differences in cross-link density, by which the higher degree of cross-linking in aldehyde-rich gels elastically

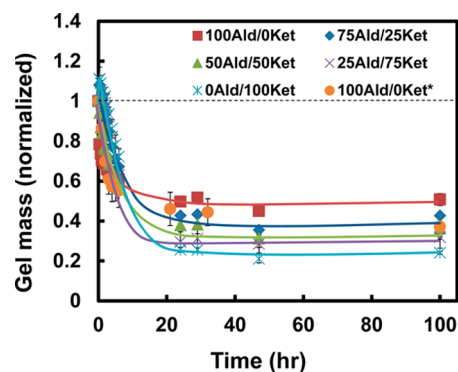


**Figure 3.** Temperature-dependent thermal collapse following gel incubation at 37 °C for PNIPAM hydrogels prepared with precursor polymers containing different aldehyde:ketone functional group ratios and different ketone functional group mole fractions (0Ald/100Ket\*  $\sim$ 42 mol % ketones; all other hydrogels  $\sim$ 12 mol % electrophile). The dashed line represents the initial mass of each hydrogel tested.

restricts gel deswelling. Interestingly, the highly functionalized 0Ald/100Ket\* gels retain their ability to thermally deswell at 37 °C to roughly the same degree as hydrogels prepared with  $\sim$ 12 mol % electrophilic group precursors despite the  $\sim$ 42 mol % ketone monomer functionalization of this precursor polymer (i.e., only  $\sim$ 58 mol % of the total monomer units are NIPAM). The slightly lower phase transition temperature of ketone-functionalized polymers relative to aldehyde polymers likely offsets the lower NIPAM content in this case. As such, based on the basis of Figure 3, the thermal phase transition can be maintained independent of the cross-link density and opacity of the hydrogel by varying both the ratio of aldehyde:ketone groups as well as the mole percentage of ketone groups in the electrophilic precursor polymer.

**Hydrogel Degradation.** Hydrogels prepared by hydrazide–ketone/aldehyde chemistry can degrade via the hydrolysis of the hydrazone cross-linking moieties, as previously demonstrated.<sup>14–16</sup> Figure 4 indicates that the rate of hydrogel degradation (as measured in PBS at 37 °C) can be tuned on the basis of the aldehyde to ketone ratio used to prepare the electrophilic precursor polymers. 0Ald/100Ket gels (containing

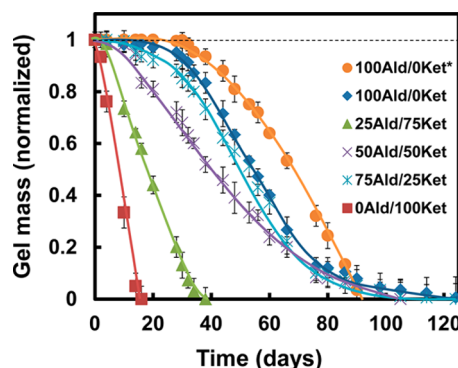


**Figure 4.** Hydrogel degradation profiles (expressed in terms of the gel mass at different time points normalized to the initial mass of the gel following co-extrusion) following gel incubation at 37 °C for PNIPAM hydrogels prepared with precursor polymers containing different aldehyde:ketone functional group ratios and different ketone functional group mole fractions (0Ald/100Ket\*  $\sim$ 42 mol % ketones; all other hydrogels  $\sim$ 12 mol % electrophile). The dashed line represents the initial mass of each hydrogel tested.

~12 mol % ketone groups and no aldehydes) degrade rapidly (~18 days) after gel formation; in contrast, 100Ald/0Ket gels (containing ~12 mol % aldehyde groups and no ketones) degrade over a much longer time period (~93 days). This difference between these two hydrogel types is likely attributable to the large observed variation in cross-linking between the two gels (Table 3), with the aldehyde-functionalized precursor polymers producing hydrogels with significantly higher cross-link densities. Of note, the 0Ald/100Ket\* hydrogel degrades more slowly than the 100Ald/0Ket hydrogel with the same cross-link density (as per  $G'$  measurements, Figure 2, and NMR, Table 3), as the extra  $\alpha$  carbon makes the hydrazone group less reactive to water hydrolysis. As such, by varying both the aldehyde:ketone ratio and the total number of ketone functional groups, the gel degradation rate can be tuned independently of the cross-link density, typically not possible with other reported injectable hydrogel formulations. Interestingly, while the 0Ald/100Ket gels undergo a nearly linear degradation profile following the onset of degradation, 100Ald/0Ket gels exhibit an additional secondary degradation profile, with a very slow degradation rate initiated at ~78 days (following >90% degradation) until complete gel degradation is achieved. These hydrogels remained as small spherical opaque samples during this secondary degradation step. This phenomenon may be attributable to the presence of inhomogeneities in these highly opaque hydrogels (see Figure 2), in which regions of higher and lower cross-link densities may be present; secondary hydrolysis may be attributable to the slower degradation of the more highly cross-linked pockets in the hydrogel. A similar secondary degradation rate was observed for gels possessing intermediate aldehyde to ketone ratios, with the effect decreasing as the ketone content is increased (and the transparency of the gel improves, see Figure 2). Furthermore, the 0Ald/100Ket\* gel that has a matched cross-link density to 100Ald/0Ket but significantly higher transparency exhibits no secondary linear region in its degradation profile, again supporting the hypothesis that an increase in ketone content in the precursor polymers leads to a greater degree of gel homogeneity and therefore a more uniform gel degradation profile.

**Polymer Cytocompatibility.** The *in vitro* cytotoxicity of the hydrogel precursor polymers, which are also the degradation products of the hydrogels,<sup>16</sup> was screened using an MTT assay with 3T3 mouse fibroblasts. Numerous previous studies from our group have shown that the PNIPAM–hydrazide component exhibits no significant cytotoxicity at the typical concentrations used in cell culture assays as well as *in vivo* in subcutaneous mouse models.<sup>14–16</sup> Therefore, the *in vitro* study herein was focused on a comparison of the cytotoxic effects of the PNIPAM–aldehyde and PNIPAM–ketone polymers, along with polymers containing a combination of aldehyde and ketone components. MTT assay results for polymers prepared with different aldehyde:ketone ratios indicated cell viabilities of at least 80% for all polymer ratios tested at concentrations up to 2 mg/mL (see the Supporting Information, Figure S4), viabilities that have been associated with little to no practical cytotoxicity.<sup>1</sup> Notably, the maximum concentration tested (2 mg/mL) is expected to be greater than the concentration of free polymer that the body would be exposed to given the relatively rapid gelation process of the hydrogels along with their slow degradation.

Figure 5 shows the results of an MTT assay performed on the 100Ald/0Ket (~12 mol % aldehydes) and 0Ald/100Ket\*

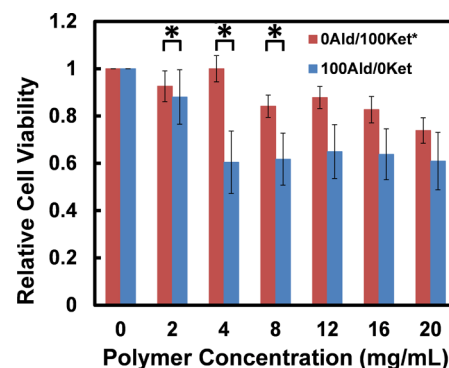


**Figure 5.** Comparison of cell viability (relative to a cell-only control) of 3T3 mouse fibroblast cells in the presence of high concentrations (>2 mg/mL) of 0Ald/100Ket\* (~42 mol % ketones) and 100Ald/0Ket (~12 mol % aldehydes). The asterisk indicates that the difference in the viabilities of the two polymers at a given concentration is statistically significant ( $p < 0.05$ ).

(~42 mol % ketones) precursor polymers at concentrations as high as 20 mg/mL (2%), a concentration typically far in excess of those screened in an *in vitro* cell culture assay. At these higher concentrations, and particularly in the range 4–12 mg/mL, the PNIPAM–ketone polymer exhibited significantly less cytotoxicity than the PNIPAM–aldehyde polymer ( $p < 0.05$ ). The PNIPAM–aldehyde polymer started to exhibit significant cytotoxicity (<80% relative viability) at concentrations above 4 mg/mL, whereas the PNIPAM–ketone polymer only exhibited equivalent cytotoxicity at a concentration of 20 mg/mL despite containing quadruple the mole fraction of electrophilic reactive functional groups. This result suggests that the use of ketones in partial or complete place of aldehydes significantly reduces the potential cytotoxicity of the precursor polymer as well as the degradation products.

## DISCUSSION

By changing the ratio of ketone to aldehyde groups in the electrophilic polymer involved in the formation of hydrazone cross-linked injectable hydrogels, significant control can be exerted over several key engineering properties of these hydrogels. The slower reactivity of ketones relative to aldehydes significantly slows the rate of gelation, increasing the time required for gel formation from several seconds in the case of aldehyde-functionalized polymers to over 1 h in the case of only ketone-functionalized polymers (Table 2). We anticipate that copolymers containing between 25 and 50 mol % ketones (yielding gelation times on the order of several minutes) may be ideal for many biomedical applications in this respect, allowing surgeons sufficient time to administer the gel at the site(s) desired while avoiding premature gelation inside the syringe. Ketone-functionalized precursor polymers also resulted in significantly more transparent hydrogels (Figure 2), a phenomenon also attributable to the slower gelation rate with these copolymers. Slower gelation allows more time for diffusional mixing of the (miscible) precursor polymers before the matrix is fixed by cross-link formation, decreasing the number of microdomain inhomogeneities within the matrix and thus leading to more transparent gels. The uniformity of hydrogels has two significant advantages in biomedical applications. First, transparency is required in some applications of hydrogels, particularly ophthalmic applications (e.g., eyedrop formulations, intraocular lenses, or vitreal substitutes) that are

particularly attractive for injectable hydrogel formulations. Second, gel uniformity reduces confounding intramatrix morphologies that may serve to complicate drug diffusion throughout the gel and simplifies the development of mathematical expressions governing drug release, improving the predictability of hydrogel performance in a drug delivery application. Similarly, if the inhomogeneities are on the same length scale as cells, local differences in cell responses to the hydrogel may result, leading to typically undesirable nonuniform cell distributions or cell behaviors within a tissue engineering matrix.

Hydrogel properties can be tuned by varying both the ratio of aldehyde:ketone groups as well as the total number of either functional group, with varying the amount of ketone groups of particular interest. Hydrogels prepared with ~42 mol % ketone-functionalized precursor polymers (0Ald/100Ket\*) maintain relatively high transparency (Figure 2) even though they gel much more quickly than even some of the more opaque hydrogels prepared using aldehyde–ketone mix precursor polymers (Table 2) and exhibit both analogous mechanical (Figure 1) and thermoresponsive properties (Figure 3) as well as slower degradation rates (Figure 4) relative to hydrogels prepared with ~12 mol % aldehyde-functionalized precursor polymers. In this way, manipulating the total number of fast (aldehyde) and slow (ketone) gelling functional groups can result in largely independent control over gelation time, gel degradation kinetics, gel transparency, hydrogel mechanics, and phase transition behavior to a degree not currently possible with existing injectable hydrogel approaches. Specifically, for all currently reported injectable hydrogel chemistries, gelation times and hydrogel degradation rates are both directly linked to the ultimate cross-link density of the hydrogel; the use of mixtures of ketones and aldehydes for hydrogel preparation decouples these parameters to provide largely independent control over multiple key hydrogel properties. This degree of control significantly improves the potential translatability of these materials in a surgical context, since hydrogels with desired mechanical properties (i.e., for matching elastic moduli of native tissues) can be delivered with a gelation time chosen by the surgeon administering the hydrogel that is most suitable to the procedure to be conducted.

Maximizing the ketone content of the precursor polymers also has demonstrated advantages in terms of maintaining high cell tolerance to the precursor polymers. Aldehyde groups can react with amine-containing cellular components via Schiff base formation, potentially disrupting regular cellular processes necessary for cell survival and proliferation (particularly at higher polymer concentrations); in comparison, ketones are inherently less reactive due to the presence of two adjacent alpha carbons instead of one, which reduces the electrophilicity of the carbonyl group and renders ketones significantly more bio-orthogonal to typical functional groups found *in vivo*.<sup>40</sup> Thus, while care must be taken not to slow the gelation time to the point where the precursor polymers diffuse away prior to gelling once injected *in vivo*, the ability to precisely tune the gelation time using ketone–aldehyde copolymers of defined compositions offers control over multiple hydrogel properties of interest. Note that all hydrogels studied in this paper are prepared with the same total mass concentration of precursor polymers (6%), a parameter that if varied would provide an additional mechanism to control the properties of the final hydrogels.

## CONCLUSIONS

Injectable hydrogels prepared by mixing hydrazide-functionalized PNIPAM with electrophilic PNIPAM precursor polymers containing mixtures of aldehyde and ketone groups can be tuned to exhibit desired gelation rates, degradation rates, opacities, and mechanical properties. Specifically, by changing the aldehyde:ketone ratio in the electrophilic polymer used for gelation and/or the mole percentage of ketones incorporated in the polymer, largely independent control over the gelation rate, opacity, degradation rate, and cross-link density can be achieved, unlike in currently reported *in situ* gelling chemistries. The hydrogels maintain their volume phase transition properties irrespective of the composition of the electrophile precursor polymer; furthermore, the presence of higher ketone fractions significantly improves the cytocompatibility of the precursor polymers (and, by extension, the degradation products) at even extremely high polymer concentrations, facilitating the use of such hydrogels in switchable biomedical applications. This chemistry approach could be applied to any synthetic or natural polymer backbone to produce highly tunable hydrogel compositions by simple mixing of well-defined precursor polymers applicable to a variety of different biomedical challenges.

## ASSOCIATED CONTENT

### Supporting Information

Schemes related to the chemistry of aldehyde monomer preparation and hydrazide polymer preparation, raw NMR data for the estimation of cross-link density in the hydrogels, and MTT assay results for electrophilic precursor polymers with different aldehyde:ketone ratios. This material is available free of charge via the Internet at <http://pubs.acs.org>.

## AUTHOR INFORMATION

### Corresponding Author

\*E-mail: [hoaretr@mcmaster.ca](mailto:hoaretr@mcmaster.ca).

### Notes

The authors declare no competing financial interest.

## ACKNOWLEDGMENTS

Funding from the 20/20: NSERC Ophthalmic Materials Research Network, the Natural Sciences and Engineering Research Council of Canada (Discovery Grants Program), and the Ontario Graduate Scholarship Program (MP) is gratefully acknowledged.

## REFERENCES

- (1) Geckil, H.; Xu, F.; Zhang, X.; Moon, S.; Demirci, U. *Nanomedicine* **2010**, *5*, 469–484.
- (2) Hoare, T. R.; Kohane, D. S. *Polymer* **2008**, *49*, 1993–2007.
- (3) Lee, K. Y.; Mooney, D. J. *Chem. Rev.* **2001**, *101*, 1869–1880.
- (4) Galperin, A.; Long, T. J.; Ratner, B. D. *Biomacromolecules* **2010**, *25*, 2583–2592.
- (5) Van Vlierberghe, S.; Dubruel, P.; Schacht, E. *Biomacromolecules* **2011**, *12*, 1387–1408.
- (6) Tan, H.; Marra, K. G. *Materials* **2010**, *3*, 1746–1767.
- (7) Nicodemus, G. D.; Bryant, S. J. *Tissue Eng., Part B* **2008**, *14*, 149–165.
- (8) Yang, W.; Xue, H.; Carr, L. R.; Wang, J.; Jiang, S. *Biosens. Bioelectron.* **2011**, *26*, 2454–2459.
- (9) Toma, M.; Jonas, U.; Mateescu, A.; Knoll, W.; Dostalek, J. *J. Phys. Chem. C* **2013**, *117*, 11705–11712.

- (10) Khimji, I.; Kelly, E. Y.; Helwa, Y.; Hoang, M.; Liu, J. *Methods* **2013**, *64*, 292–298.
- (11) Hiemstra, C.; van der Aa, L. J.; Zhong, Z.; Dijkstra, P. J.; Feijen, J. *Biomacromolecules* **2007**, *8*, 1548–1556.
- (12) Azab, A. K.; Doviner, V.; Orkin, B.; Kleinstern, J.; Srebnik, M.; Nissan, A.; Rubinstein, A. *J. Biomed. Res., Part A* **2007**, *2*, 414–422.
- (13) Guvendiren, M.; Lu, H. D.; Burdick, J. A. *Soft Matter* **2012**, *8*, 260.
- (14) Campbell, S. B.; Patenaude, M.; Hoare, T. *Biomacromolecules* **2013**, *14*, 644–653.
- (15) Patenaude, M.; Hoare, T. *Biomacromolecules* **2012**, *13*, 369–378.
- (16) Patenaude, M.; Hoare, T. *ACS Macro Lett.* **2012**, *1*, 409–413.
- (17) Pritchard, C. D.; O'Shea, T. M.; Siegwart, D. J.; Calo, E.; Anderson, D. G.; Reynolds, F. M.; Thomas, J.; Slotkin, J. R.; Woodard, E. J.; Langer, R. *Biomaterials* **2011**, *32*, 587–597.
- (18) Yu, Y.; Deng, C.; Meng, F.; Shi, Q.; Feijen, J.; Zhong, Z. *J. Biomed. Mater. Res., Part A* **2011**, *99*, 316–326.
- (19) Sekine, Y.; Moritani, Y.; Ikeda-Fukazawa, T.; Sasaki, Y.; Akiyoshi, K. *Adv. Healthcare Mater.* **2012**, *1*, 722–728.
- (20) Censi, R.; Fieten, P. J.; Di Martino, P.; Hennink, W. E.; Vermonden, T. *J. Controlled Release* **2010**, *148*, 28–29.
- (21) Wei, H. L.; Yang, Z.; Zheng, L. M.; Shen, Y. M. *Polymer* **2009**, *50*, 2836–2840.
- (22) Nimmo, C. M.; Owen, S. C.; Shoichet, M. S. *Biomacromolecules* **2011**, *12*, 824–830.
- (23) Tan, H.; Rubin, J. P.; Marra, K. G. *Macromol. Rapid Commun.* **2011**, *32*, 905–911.
- (24) Grover, G. N.; Lam, J.; Nguyen, T. H.; Segura, T.; Maynard, H. D. *Biomacromolecules* **2012**, *13*, 3013–3017.
- (25) Vetrík, M.; Příkladný, M.; Hrubý, M.; Michálek, J. *Polym. Degrad. Stab.* **2011**, *96*, 756–759.
- (26) Sivakumaran, D.; Maitland, D.; Hoare, T. *Biomacromolecules* **2011**, *12*, 4112–4120.
- (27) Ito, T.; Yeo, Y.; Highley, C. B.; Bellas, E.; Kohane, D. S. *Biomaterials* **2007**, *28*, 3418–3426.
- (28) Beauchamp, R. O.; Clair, M. B.; St; Fennell, T. R.; Clarke, D. O.; Morgan, K. T.; Kari, F. W. *Crit. Rev. Toxicol.* **1992**, *22*, 143–174.
- (29) Gough, J. E.; Scotchford, C.; Downes, S. *J. Biomed. Mater. Res.* **2002**, *61*, 121–130.
- (30) O'Brien, P. J.; Siraki, A. G.; Shangari, N. *Crit. Rev. Toxicol.* **2005**, *35*, 609–662.
- (31) Meid, J.; Friedrich, T.; Tieke, B.; Lindner, P.; Richtering, W. *Phys. Chem. Chem. Phys.* **2011**, *13*, 3039–3047.
- (32) McKinnon, D. D.; Domaille, D. W.; Cha, J. N.; Anseth, K. S. *Adv. Mater.* **2013**, DOI: 10.1002/adma.201303680.
- (33) Uzu, S.; Kanda, S.; Imai, K. *Analyst* **1990**, *115*, 1477–1482.
- (34) Cai, S.; Suo, Z. *J. Mech. Phys. Solids* **2011**, *59*, 2259–2278.
- (35) Kang Derwent, J. J.; Mieler, W. F. *Trans. Am. Ophthalmol. Soc.* **2008**, *106*, 206–213.
- (36) Hou, Y.; Matthews, A. R.; Smitherman, A. M.; Bulick, A. S.; Hahn, M. S.; Hou, H.; Han, A.; Grunlan, M. *Biomaterials* **2008**, *29*, 3175–3184.
- (37) Adachi, J.; Sato, N. *J. Org. Chem.* **1972**, *37*, 221–225.
- (38) Motokawa, R.; Morishita, K.; Koizumi, S.; Nakahira, T.; Annaka, M. *Macromolecules* **2005**, *38*, 5748–5760.
- (39) Dong, Y.; Hassan, W.; Zheng, Y.; Saeed, A. O.; Cao, H.; Tai, H.; Pandit, A.; Wang, W. *J. Mater. Sci.: Mater. Med.* **2012**, *23*, 25–35.
- (40) Sletten, E. M.; Bertozzi, C. R. *Angew. Chem., Int. Ed.* **2009**, *38*, 6974–6998.